Log-aesthetic curves and generalized Archimedean spirals

Péter Salvi

Budapest University of Technology and Economics, Hungary

Abstract

We show that the radials of log-aesthetic curves are generalized Archimedean spirals. Examining the logarithmic curvature histogram reveals that these radials have an inherent similarity to the associated log-aesthetic curves, and can also be used as computationally inexpensive approximants. Different kinds of fits are proposed and discussed through examples. A possible generalization of log-aesthetic curves based on generalized Archimedean spirals is also explored.

Keywords: log-aesthetic curve, generalized Archimedean spiral, radial curve, approximation

1. Introduction

One of the basic goals of computer-aided design (CAD) is to create beautiful objects, possessing 'nice' feature curves. The aesthetics are usually measured by various *fairness measures*, generally based on (the variation of) curvature.

While post-processing methods and variational fairing are the staples of modern CAD systems, there is another strand of research, primarily concerned with such representations that are fair by definition.

In a seminal work, Harada et al. (1999) analyzed the *logarithmic curvature histogram* (LCH) of various curves and identified fair curves as those represented by straight segments. Miura (2006) defined *log-aesthetic* (LA) curves exactly by this characteristic.

The class of LA curves contains several classical curves, such as the clothoid, the logarithmic spiral, and the circle involute. A drawback of this representation is, however, that it is given as an integral expression for which no closed form exists.

In this work we prove that there is a close relationship between LA curves and generalized Archimedean (GA) spirals, which—to the best knowledge of the author—has not been understood before. It is also shown that GA spirals are suitable as a computationally inexpensive approximation of LA curves. Additionally, a possible generalization of the log-aesthetic class of curves is investigated, as well, based on GA spirals.

The paper is structured as follows. After briefly reviewing the relevant literature in Section 2, we summarize some basic facts about LA curves and GA spirals in Section 3; the relationship between the two is analyzed in Section 4. Approximation of LA curves by GA spirals is treated in Section 5. Finally, a broader class of aesthetic curves is proposed in Section 6.

2. Previous work

There seem to be no precedent of looking at radials of LA curves; their evolutes, however, were shown to be LA curves by Yoshida and Saito (2012). The same authors analyzed the LCH slopes of some GA spirals (among other curves) in Yoshida and Saito (2024), in particular the lituus, the hyperbolic spiral, the arithmetic spiral, and Fermat's spiral.

There have been several papers on the approximation of LA curves, usually by polynomials (e.g. Yoshida et al., 2013; Lu and Xiang, 2016; Tsuchie and Yoshida, 2022), but also other representations (Miura et al., 2007; Albayari et al., 2023).

Our main contribution is the exact relationship of GA spirals to LA curves, and their use as both approximations and a new basis for aesthetic curves.

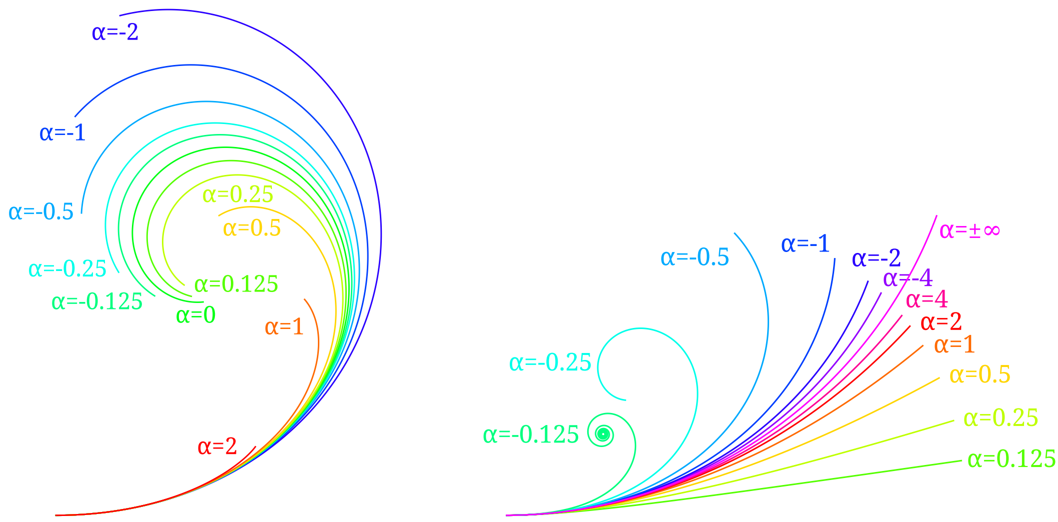

Figure 1: Log-aesthetic curves with various α values. Left: with $\kappa_{\mathrm{LA}}(0) = \kappa'_{\mathrm{LA}}(0) = 1$ (and thus different c_0, c_1, c_2 parameters). Right: with $c_0 = c_1 = 1$.

3. Preliminaries

Here we summarize some important properties of LA curves and GA spirals.

3.1. LA curves

LA curves are defined by their curvature as a function of arc length:

$$\kappa_{\mathrm{LA}}(s) = (c_0 s + c_1)^{-\frac{1}{\alpha}}, \tag{1}$$

where α, c_0 and c_1 are suitable constants. The angle between the tangent and the x axis can be computed by integrating Eq. (1):

$$\theta_{\mathrm{LA}}(s) = \frac{\alpha(c_0 s + c_1)^{\frac{\alpha-1}{\alpha}}}{(\alpha - 1)c_0} + c_2. \tag{2}$$

(In the case of $\alpha \in \{0, 1\}$ these equations are slightly different, see e.g. Salvi (2026).)

The curve itself is then given by

$$\mathbf{C}_{\mathrm{LA}}(s) = \mathbf{P}_0 + \left[\int_0^s \cos\theta_{\mathrm{LA}}(s)\,\mathrm{d}s, \int_0^s \sin\theta_{\mathrm{LA}}(s)\,\mathrm{d}s\right]. \tag{3}$$

Since we only care about the *shape* now, the starting point and angle (controlled by $\mathbf{P}_0$ and c_2, respectively) are irrelevant and can be set arbitrarily. Throughout the paper we use the convention of $\mathbf{C}_{\mathrm{LA}}(s_{\min}) = \mathbf{0}$ and $\theta_{\mathrm{LA}}(s_{\min}) = 0$, so a curve segment $[s_{\min}, s_{\max}]$ always begins at the origin, and its tangent points to the right.

We will also need the derivative of the curvature later on:

$$\kappa'_{\mathrm{LA}}(s) = -\frac{1}{\alpha} \cdot c_0(c_0 s + c_1)^{-\frac{1+\alpha}{\alpha}}. \tag{4}$$

Figure 1 shows some examples. The common characteristic of these curves is that their LCH graph is a straight line with slope α.

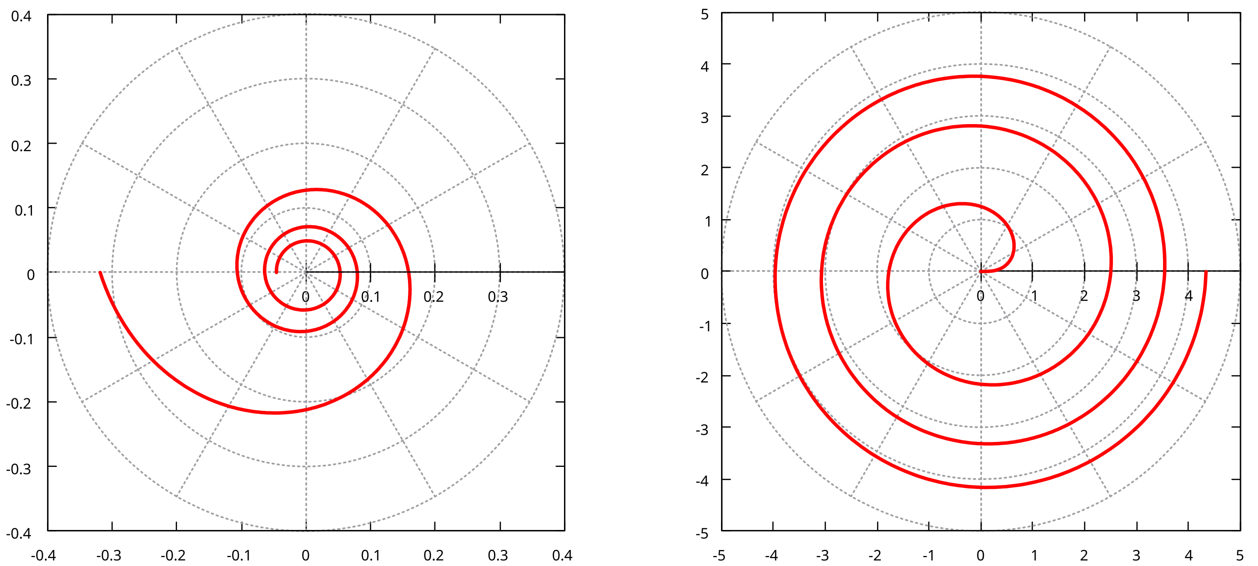

Figure 2: Two generalized Archimedean spirals with $a = 0$ and $b = 1$. Left: hyperbolic spiral ($c = -1$), $t \in [\pi, 7\pi]$. Right: Fermat's spiral ($c = 2$), $t \in [0, 6\pi]$.

3.2. GA spirals

GA spirals are given by the polar equation

$$r = a + b\phi^{\frac{1}{c}}, \tag{5}$$

where (r, ϕ) are the polar coordinates (see Fig. 2). This is the usual formulation (see e.g. Diedrichs, 2019), although slightly different variations, like the one in Miura et al. (2019), also exist. In other words, the parametric equation of the curve, with $t = \phi$, is[1]

$$\mathbf{C}_{\mathrm{GA}}(t) = [\cos t, \sin t] \cdot (a + bt^{\frac{1}{c}}). \tag{6}$$

We will mainly focus on the subclass where $a = 0$; quantities associated with these spirals will be marked by a hat. Curvature is computed as

$$\hat{\kappa}_{\mathrm{GA}}(t) = \left|\frac{c}{b}\right| \cdot t^{\frac{c-1}{c}} \cdot \frac{c^2t^2 + c + 1}{(c^2t^2 + 1)^{\frac{3}{2}}}, \tag{7}$$

and the derivative of its arc length is

$$\hat{s}'_{\mathrm{GA}}(t) = \left|\frac{b}{c}\right| \cdot t^{\frac{1-c}{c}} \sqrt{c^2t^2 + 1}. \tag{8}$$

The derivative of curvature is

$$\hat{\kappa}'_{\mathrm{GA}}(t) = -\left|\frac{c}{b}\right| \cdot \frac{c^4t^4 + 2c^4t^2 + 2c^2t^2 - c^2 + 1}{ct^{\frac{1}{c}}(c^2t^2 + 1)^{\frac{5}{2}}}, \tag{9}$$

so the derivative w.r.t. arc length is given by

$$\frac{\hat{\kappa}'_{\mathrm{GA}}(t)}{\hat{s}'_{\mathrm{GA}}(t)} = -\frac{c}{b^2} \cdot t^{\frac{c-2}{c}} \cdot \frac{c^4t^4 + 2c^4t^2 + 2c^2t^2 - c^2 + 1}{(c^2t^2 + 1)^3}. \tag{10}$$

Straightforward computation shows that these curves have monotonic curvature when $(t^2 + 1)c^2 \geq |c|\sqrt{c^2 + 3}$, and for $c < -1$ they have an inflection point at $t = \sqrt{-(c + 1)/c^2}$.

[1] In a polar equation we refer to the angle as ϕ, while we denote it with t when used as a running parameter.

```
declare(t, real)$ assume(t > 0)$          /* the parameter t is a positive real        */
p:   exp(%i * t) * (a + b * t^(1 / c))$   /* point of the curve at parameter t         */
dp:  diff(p, t)$                          /* first derivative                          */
ddp: diff(dp, t)$                         /* second derivative                         */
ds:  trigsimp(cabs(dp))$                  /* first derivative of arc length            */
dds: factor(diff(ds, t))$                 /* second derivative of arc length           */
k:   imagpart(conjugate(dp) * ddp) / ds^3$ /* curvature                                */
r:   trigsimp(1 / k)$                     /* radius of curvature                       */
dr:  factor(diff(r, t))$                  /* first derivative of radius of curvature   */
ddr: factor(diff(dr, t))$                 /* second derivative of radius of curvature  */
alp: 1 + r / dr^2 * (dr * dds / ds - ddr)$ /* alpha (LCH slope)                        */
factor(ev(alp, [a = 0]));
```

Figure 3: Maxima program for computing Eq. (16).

4. Radials of LA curves

The radial of a curve is the vector to the center of curvature, placed at the origin:

$$\mathbf{R}(t) = [\cos\theta^{\perp}(t), \sin\theta^{\perp}(t)] \cdot \rho(t) = \left[\cos\left(\theta(t) + \frac{\pi}{2}\right), \sin\left(\theta(t) + \frac{\pi}{2}\right)\right] \cdot \rho(t), \tag{11}$$

where $\rho(t) = 1/\kappa(t)$ is the radius of curvature, and $\theta^{\perp}(t)$ is the normal angle, measured from the x axis.

We want to prove that the radial of a LA curve is a GA spiral. A well-known example is that the *lituus* (GA spiral with $c = -2$) is the radial of the *clothoid* or *Euler spiral* (LA curve with $\alpha = -1$). In the following we show that this relationship is true in general, i.e., the radial is a GA spiral with $c = \alpha - 1$.

From Eq. (2) we have

$$s_{\mathrm{LA}}(\theta) = \frac{1}{c_0}\left((\theta - c_2)c_0\frac{\alpha-1}{\alpha}\right)^{\frac{\alpha}{\alpha-1}} - \frac{c_1}{c_0}. \tag{12}$$

The constant c_2 just rotates the curve and can be chosen arbitrarily. Let us set it to $-\frac{\pi}{2}$, and express the radius of curvature as a function of θ:

$$\rho_{\mathrm{LA}}(\theta) = (c_0 s_{\mathrm{LA}}(\theta) + c_1)^{\frac{1}{\alpha}} = \left(\left(\theta + \frac{\pi}{2}\right)c_0\frac{\alpha-1}{\alpha}\right)^{\frac{1}{\alpha-1}}. \tag{13}$$

The polar equation of the radial curve, with $r = \rho_{\mathrm{LA}}(\theta)$ and $\phi = \theta^{\perp} = \theta + \frac{\pi}{2}$, is consequently

$$r = \left(\phi \cdot c_0\frac{\alpha-1}{\alpha}\right)^{\frac{1}{\alpha-1}} = \left(c_0\frac{\alpha-1}{\alpha}\right)^{\frac{1}{\alpha-1}}\phi^{\frac{1}{\alpha-1}}, \tag{14}$$

which is of the form of Eq. (5) with $a = 0$ and $c = \alpha - 1$.

Let us see the two special cases. For Nielsen's spiral ($\alpha = 0$), the same reasoning shows that the radial is a hyperbolic spiral $r = \frac{1}{c_0}\phi^{-1}$, as expected. The only real exception is the logarithmic spiral ($\alpha = 1$) – here the radial is also a logarithmic spiral: $r = e^{c_0\phi}$.

5. Radials as approximants

In this section we show that these radial curves also serve as computationally inexpensive approximants to the corresponding LA curves. For example, it is common knowledge (see e.g. Barbero and Ritoré, 2019) that the *arithmetic spiral* (GA spiral with $c = 1$) is very similar to the *circle involute* (LA curve with $\alpha = 2$).

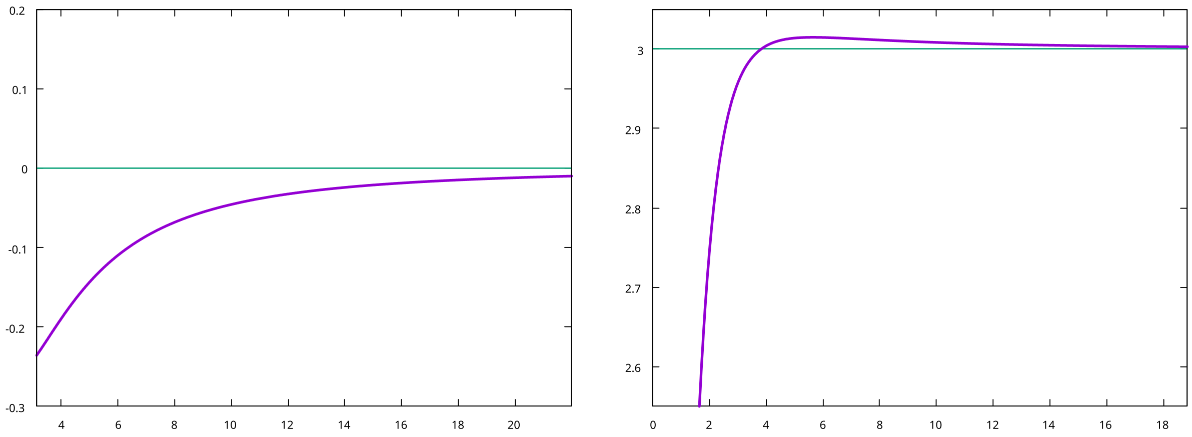

Figure 4: Typical LCH graphs of GA spirals for the $c < 1$ and $c > 1$ cases, corresponding to the examples in Figure 2.

5.1. *LCH slope of GA spirals*

As discussed in Section 3, the logarithmic curvature histogram of a LA curve is a straight line with slope given by α. In general, the slope can be computed as in Gobithaasan and Miura (2014):

$$\alpha(t) = 1 + \frac{\rho(t)}{\rho'(t)^2}\left(\frac{\rho'(t)s''(t)}{s'(t)} - \rho''(t)\right) = 1 - \frac{\rho(s)\rho''(s)}{\rho'(s)^2}, \tag{15}$$

which, in the case of GA spirals with $a = 0$ becomes

$$\begin{aligned}\hat{\alpha}_{\mathrm{GA}}(t) = (&c^9t^8 + c^8t^8 + 6c^9t^6 + c^8t^6 + 4c^7t^6 + 4c^6t^6 + 2c^8t^4 - c^7t^4 + c^6t^4 + 6c^5t^4 + 6c^4t^4 - 7c^6t^2 - 8c^5t^2 \\ &- c^4t^2 + 4c^3t^2 + 4c^2t^2 - c^3 - c^2 + c + 1)\,/\,(c^4t^4 + 2c^4t^2 + 2c^2t^2 - c^2 + 1)^2,\end{aligned} \tag{16}$$

as computed by the Maxima program in Figure 3. The leading term is $(c + 1)c^8t^8$ in the numerator, and c^8t^8 in the denominator, so

$$\lim_{t\to\infty} \hat{\alpha}_{\mathrm{GA}}(t) = c + 1. \tag{17}$$

As we have seen in the previous section, $c = \alpha - 1$ for the radial curve. This means that in general the LCH slope of the radial of a LA curve approaches the same α value as the curve itself, and consequently, for sufficiently large t, the radial is a good approximation of the LA curve. Note that the slope does not depend on the b parameter. Typical slope graphs are shown in Figure 4.

5.2. *Approximation*

For a LA curve segment given by $\{\alpha, c_0, c_1\}$ parameters and an $[s_{\min}, s_{\max}]$ interval, we want to find an approximating segment of a GA spiral with $a = 0$ and $c = \alpha - 1$. Let us assume that we have already selected a starting parameter $t_{\min}$. Then we can interpolate the curvature at $t_{\min}$ by setting b (see Eq. 7):

$$b = \frac{1}{\kappa_{\mathrm{LA}}(s_{\min})} \cdot |c| \cdot t_{\min}^{\frac{c-1}{c}} \cdot \frac{c^2t_{\min}^2 + c + 1}{(c^2t_{\min}^2 + 1)^{\frac{3}{2}}}. \tag{18}$$

How should we choose $t_{\min}$? A straightforward option is to require that the derivative of curvature by arc length (Eq. 10) also matches that of the LA curve (Eq. 4). This is achieved by a simple binary search; the initial frame can be found by iterative doubling. Figure 5 shows some examples.

Depending on the application, it may be more practical to interpolate the endpoint, even if it incurs larger deviations near the beginning of the curve. We set b as above, but the bisection uses a different error function to find $t_{\min}$, computed by the following steps:

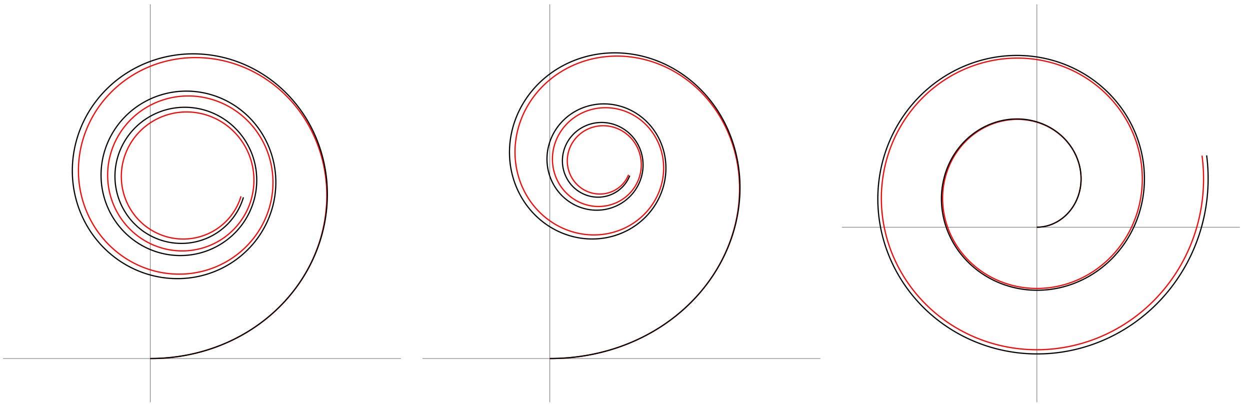

Figure 5: Approximations of LA curves (red: LA curve; black: GA spiral). Left: $\alpha = -1$, $c_0 = 2$, $c_1 = 2.8$, $s_{\min} = 0$. Middle: $\alpha = 0$, $c_0 = 0.8$, $c_1 = 0.6$, $s_{\min} = 0.4$. Right: $\alpha = 2$, $c_0 = 0.7$, $c_1 = 1.5$, $s_{\min} = 0.6$.

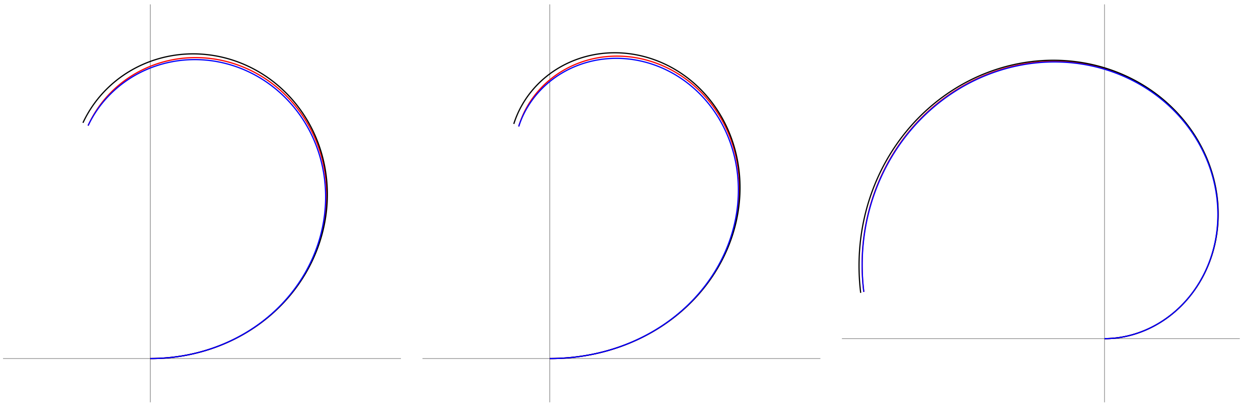

Figure 6: Approximations with endpoint interpolation on the same examples as in Figure 5, but shorter intervals (red: LA curve; black: the fit in Fig. 5; blue: endpoint interpolating fit). Left: $s_{\max} = 1.1$. Middle: $s_{\max} = 1.5$. Right: $s_{\max} = 11.4$.

1. Rotate the spiral s.t. $\mathbf{C}'_{\mathrm{GA}}(t_{\min})$ points to the right.
2. Set $\mathbf{Q}$ (the spiral center) s.t. $\mathbf{Q} + \mathbf{C}_{\mathrm{GA}}(t_{\min}) = \mathbf{0}$.
3. Let $\mathbf{u}$ and $\mathbf{v}$ be unit vectors from $\mathbf{Q}$ to $\mathbf{0}$ and $\mathbf{C}_{\mathrm{LA}}(s_{\max})$, respectively.
4. Set $t_{\max} = t_{\min} + \arccos\langle \mathbf{u}, \mathbf{v} \rangle$, or, if $\det(\mathbf{u}, \mathbf{v}) < 0$, choose the larger angle: $t_{\max} = t_{\min} + 2\pi - \arccos\langle \mathbf{u}, \mathbf{v} \rangle$.
5. The error is $\|\mathbf{C}_{\mathrm{LA}}(s_{\max}) - \mathbf{Q}\| - \|\mathbf{C}_{\mathrm{GA}}(t_{\max})\|$.

This algorithm assumes that $t_{\max} - t_{\min} < 2\pi$, but it is easy to extend it to other cases, as well. Some examples are shown in Figure 6.

Since the curvature at $s_{\min}$ is interpolated in both versions of the approximation, these can also be used to build G^2-continuous spline curves consisting of GA spiral segments. The primary advantage emerges, however, when long segments can be closely fitted by a single spiral. For the conditions enabling this, refer to the next section.

5.3. Limitations

When $t_{\min}$ is relatively large, the fit works very well (as expected, considering the LCH slopes seen at the beginning of this section). The left image in Figure 7 shows such an example ($t_{\min} \approx 9.88$); the two curves are virtually identical. The right figure shows the other extreme ($t_{\min} \approx 1.42$), where only a very short segment is approximated tightly. Still, most practical applications need only relatively short segments, so this should not be a very serious issue.

Table 1 shows the deviations in some characteristic cases. The shape parameter α is set to several representative values between -2 and 2, while the starting parameter $s_{\min}$ is chosen such that the tangent angle is at that point a given

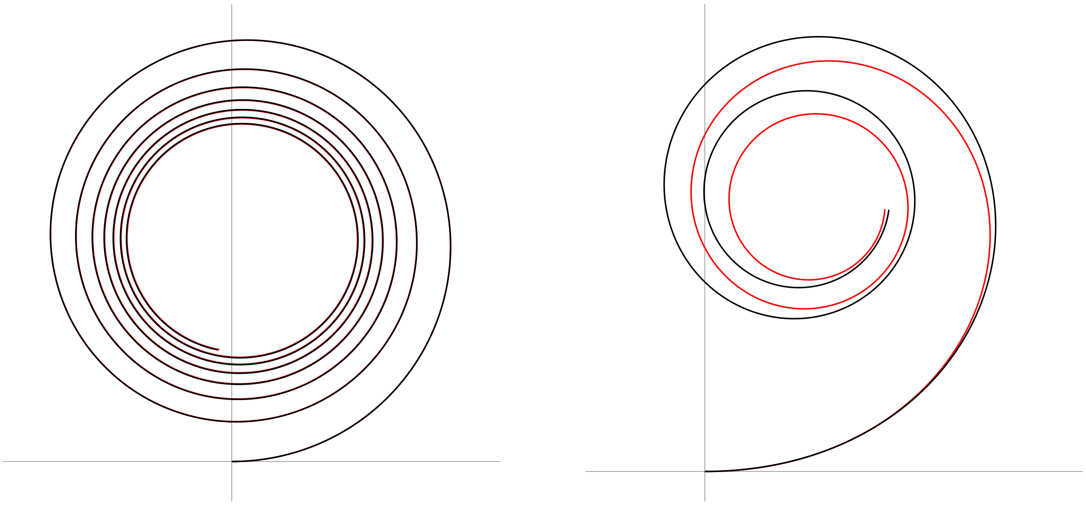

Figure 7: Good and bad approximations. Left: $\alpha = -1.5$, $c_0 = 2$, $c_1 = 2.8$, $s_{\min} = 2.6$. Right: $\alpha = -1$, $c_0 = 1$, $c_1 = 1$, $s_{\min} = 0$.

	$\alpha = -2$	$\alpha = -3/2$	$\alpha = -1$	$\alpha = -1/2$	$\alpha = 0$	$\alpha = 3/2$	$\alpha = 2$
$\theta_0 = 0$	1.82	1.61	1.38	1.13	2.50	1.35	1.48
$\theta_0 = \pi/4$	2.61	2.35	2.03	1.69	2.99	1.94	2.62
$\theta_0 = \pi/2$	3.31	3.06	2.73	2.29	3.43	2.52	3.82
$\theta_0 = 3\pi/4$	4.09	3.73	3.33	2.89	3.89	3.13	4.79
$\theta_0 = \pi$	4.78	4.44	3.99	3.42	4.37	3.77	$> 2\pi$
$\theta_0 = 5\pi/4$	5.40	5.04	4.61	4.00	4.79	4.34	$> 2\pi$
$\theta_0 = 3\pi/2$	6.03	5.62	5.15	4.56	5.19	4.80	$> 2\pi$
$\theta_0 = 7\pi/4$	$> 2\pi$	6.22	5.68	5.05	5.58	5.59	$> 2\pi$
$\theta_0 = 2\pi$	$> 2\pi$	$> 2\pi$	6.24	5.51	5.97	6.25	$> 2\pi$

Table 1: Maximum interpolating interval (in polar angles) below a relative error of 10^{-3}, with various α values, starting at given tangent angles. The rest of the parameters are set as on the right-hand side of Fig. 1, i.e., with $c_0 = c_1 = 1$.

ratio ($\ell/8$) of a full turn, i.e., $\theta(s_{\min}) = \ell/8 \cdot 2\pi$, $\ell = 0 \ldots 8$. These values are selected because if $s_{\min}$ gets even larger, log-aesthetic curves get more and more similar to circular arcs, which renders the problem less interesting. The values in the table show the maximum of $t_{\max} - t_{\min}$, as computed by the second approximation method above, while keeping the maximum error relative to the axis aligned bounding rectangle diagonal below a fixed tolerance (10^{-3}).

Deviations are computed between dense samples (10000 points per curve), giving slightly lower bounds. The actual values also depend on the chosen tolerance, but the trends are clear. As expected, we can approximate longer and longer segments as $s_{\min}$ grows; the lowest values are obtained consequently when we approximate the beginning of LA curves. It can be seen that larger $|\alpha|$ values are fitted better; the exception here is $\alpha = 0$, Nielsen's spiral, whose fit is particularly good. (Note that the logarithmic spiral ($\alpha = 1$) is not included, as it does not have a GA spiral counterpart, and the $\alpha = 1/2$ case is omitted because it quickly approaches a straight line.)

Another (technical) difficulty is that when $|\alpha| < 1$ the computations may require handling very large numbers, but this is a peculiarity of the LA curve representation.

6. Inverse radials of GA spirals

We can define the inverse relation: we seek a curve $\mathbf{C}(t)$ whose radial is a given $\mathbf{R}(t)$ curve (modulo rigid transformations). This in itself does not contain enough information, but it is easy to see that in the case of LA curves, the

```
dx:  -sin(t) * t^(1 / c)$                      /* first derivative of curve by ...      */
dy:  cos(t) * t^(1 / c)$                       /* ... (-y, x) coordinates of the radial */
ds:  trigsimp(sqrt(dx^2 + dy^2))$              /* first derivative of arc length        */
dds: diff(ds, t)$                              /* second derivative of arc length       */
ddx: diff(dx, t)$ ddy: diff(dy, t)$            /* second derivative of the curve        */
r:   trigsimp(ds^3 / (dx * ddy - dy * ddx))$   /* radius of curvature                   */
dr:  diff(r, t)$                               /* 1st derivative of radius of curvature */
ddr: diff(dr, t)$                              /* 2nd derivative of radius of curvature */
alp: 1 + r / dr^2 * (dr * dds / ds - ddr)$     /* alpha (LCH slope)                     */
factor(alp);
```

Figure 8: Maxima program for checking the LCH slope of reconstructed LA curves.

radial is parameterized in a way that $\|\mathbf{C}'(t)\| = \|\mathbf{R}(t)\|$. Then

$$\mathbf{C}(t) = \int_0^t \begin{bmatrix} 0 & -1 \\ 1 & 0 \end{bmatrix} \cdot \mathbf{R}(t)\,\mathrm{d}t. \tag{19}$$

To double-check, we can make a quick computation (Fig. 8) that shows that the reconstructed curve *does* have a constant LCH slope of $c + 1$.

The class of curves reconstructed from GA spirals trivially includes LA curves. Note that for $a = 0$, $b = 1$, $c = 1$ this gives the common equation for the circle involute:

$$\mathbf{C}_{\alpha:2}(t) = \int_0^t [-t\sin t, t\cos t]\,\mathrm{d}t = [t\cos t - \sin t, t\sin t + \cos t]. \tag{20}$$

What is more interesting, with this change of variable, we obtain explicit equations for other LA curves, as well. For example, for $\alpha = \frac{3}{2}$ we have $c = \frac{1}{2}$, resulting in

$$\mathbf{C}_{\alpha:\frac{3}{2}}(t) = [(t^2 - 2)\cos t - 2t\sin t, (t^2 - 2)\sin t + 2t\cos t]. \tag{21}$$

Even for clothoids ($\alpha = -1$) an expression involving incomplete gamma functions becomes readily available (also proposed before in Ziatdinov et al., 2012).

6.1. *From GA spirals to generalized LA curves*

In the case of arithmetic spirals ($c = 1$) the a parameter just shifts the curve, so the radial inverse is a circle involute.

For $c < 0$, a simple analysis of the leading coefficients in the LCH slope equation, similarly to that of the previous section, reveals that in the presence of $a \neq 0$ the slope diverges into (positive or negative) infinity.

For $c > 0$, however, the limit of the LCH slope is still $c + 1$. Since these are distinct from the $a = 0$ spirals, the radial inverses of such curves are not LA curves, but still have a nice curvature distribution, and can be regarded as aesthetic curves. Two examples with various a values are shown in Figure 9.

Conclusion

We have shown that log-aesthetic curves and generalized Archimedean spirals have a very close relationship:

- The radial of a LA curve is a GA spiral
- Such radials have a LCH slope that approaches that of the corresponding LA curve
- GA spirals can be used to approximate LA curves

LA curves can be reconstructed from their radials; this fact led us to derive explicit equations for some LA curves, and also to define a broader class of aesthetic curves.

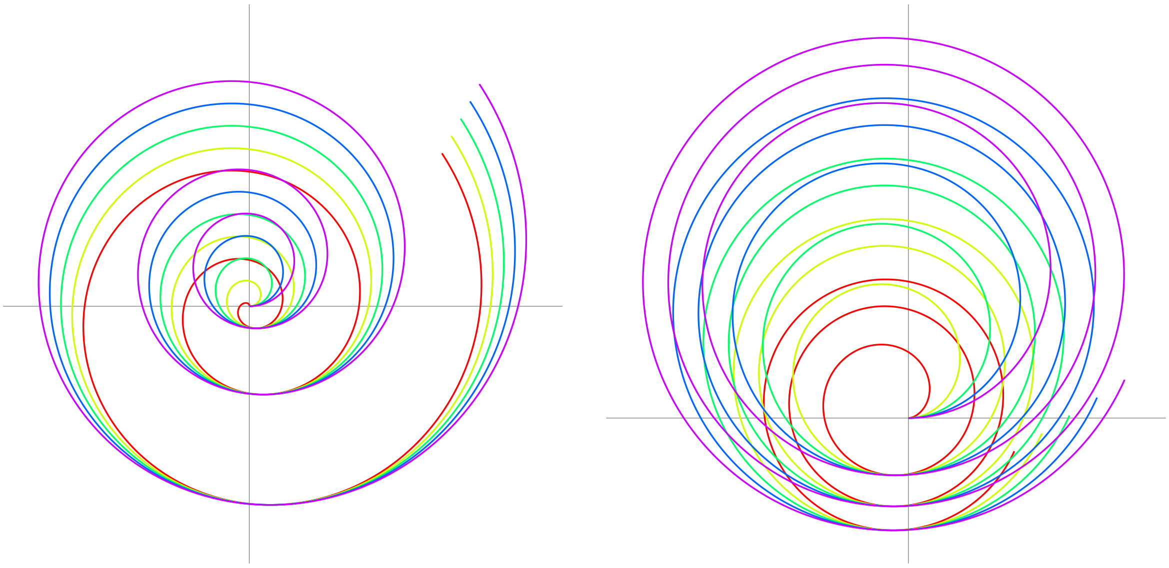

Figure 9: Generalized LA curves with $b = 1$ and various a values; the original LA curves are red. Left: $c = 0.5$, $a \in \{0, 20, 40, 60, 80\}$. Right: $c = 2$, $a \in \{0, 1, 2, 3, 4\}$.

Acknowledgments

This project has been supported by the Hungarian Scientific Research Fund (OTKA, No. 145970). The author would like to thank the anonymous reviewers for their insightful comments, which have greatly contributed to improving the paper.

References

Albayari, D., Gobithaasan, R.U., Miura, K.T., 2023. The approximation of generalized log-aesthetic curves with G^2 cubic trigonometric Bézier function. Journal of Mathematics 2023, 7457223. doi:10.1155/2023/7457223.

Barbero, S., Ritoré, M., 2019. Circle involute as an optimal scan path, minimizing acquisition time, in surface topography. Surface Topography: Metrology and Properties 7, 035010. doi:10.1088/2051-672X/ab3706.

Diedrichs, D.R., 2019. Archimedean, logarithmic and Euler spirals – Intriguing and ubiquitous patterns in nature. The Mathematical Gazette 103, 52–64. doi:10.1017/mag.2019.7.

Gobithaasan, R.U., Miura, K.T., 2014. Logarithmic curvature graph as a shape interrogation tool. Applied Mathematical Sciences 8, 755–765. doi:10.12988/ams.2014.312709.

Harada, T., Yoshimoto, F., Moriyama, M., 1999. An aesthetic curve in the field of industrial design, in: Proceedings of IEEE Symposium on Visual Language, pp. 38–47. doi:10.1109/VL.1999.795873.

Lu, L., Xiang, X., 2016. Quintic polynomial approximation of log-aesthetic curves by curvature deviation. Journal of Computational and Applied Mathematics 296, 389–396. doi:10.1016/j.cam.2015.10.002.

Miura, K.T., 2006. A general equation of aesthetic curves and its self-affinity. Computer-Aided Design and Applications 3, 457–464. doi:10.1080/16864360.2006.10738484.

Miura, K.T., Fujisawa, M., Kobayashi, K.G., Cheng, F., 2007. 3D extension of aesthetic plane curve and its B-spline approximation, in: Proceedings of the CAD Conference.

Miura, K.T., Usuki, S., Sekine, T., 2019. An extension of algebraic spiral including Archimedes, Fermat, lituus and hyperbolic spirals and its properties, in: Proceedings of JSPE Semestrial Meeting, In Japanese. pp. 679–680. doi:10.11522/pscjspe.2019A.0_679.

Salvi, P., 2026. Generalized catenaries and trig-aesthetic curves. Computer-Aided Design and Applications 23, 56–67. doi:10.14733/cadaps.2026.56-67.

Tsuchie, S., Yoshida, N., 2022. High-quality approximation of log-aesthetic curves based on the fourth-order derivative. Journal of Computational Design and Engineering 9, 2439–2451. doi:10.1093/jcde/qwac117.

Yoshida, N., Fukuda, R., Saito, T., Saito, T., 2013. Quasi-log-aesthetic curves in polynomial Bézier form. Computer-Aided Design and Applications 10, 983–993. doi:10.3722/cadaps.2013.983-993.

Yoshida, N., Saito, T., 2012. The evolutes of log-aesthetic planar curves and the drawable boundaries of the curve segments. Computer-Aided Design and Applications 9, 721–731. doi:10.3722/cadaps.2012.721-731.

Yoshida, N., Saito, T., 2024. Shape information of curves and its visualization using two-tone pseudo coloring. Computer-Aided Design and Applications 21, 11–28. doi:10.14733/cadaps.2024.11-28.

Ziatdinov, R., Yoshida, N., Kim, T.W., 2012. Analytic parametric equations of log-aesthetic curves in terms of incomplete gamma functions. Computer Aided Geometric Design 29, 129–140. doi:10.1016/j.cagd.2011.11.003.